



Pergamon

PYRROLES AND OTHER HETEROCYCLES AS INHIBITORS OF P38 KINASE

Stephen E. de Laszlo^a, Denise Visco^b, Lily Agarwal^b, Linda Chang, Jayne Chin^a, Gist Croft^a, Amy Forsyth^b, Daniel Fletcher^b, Betsy Frantz^a, Candice Hacker, William Hanlon^a, Coral Harper^a, Matthew Kostura^a, Bing Li, Sylvie Luell^b, Malcolm MacCoss, Nathan Mantlo¹, Edward A. O'Neill^a, Chad Oreillo^b, Margaret Pang^a, Janey Parsons^a, Anna Rolando^a, Yousif Sahly^c, Kelley Sidler, W. Rick Widmer^d and Stephen J. O'Keefe^a

Departments of Medicinal Chemistry, Inflammation Research^a and Pharmacology,^b Merck Research Laboratories, Rahway, NJ, 07065, U.S.A. Department of Drug Metabolism,^c Merck Research Laboratories, West Point, PA, 19486, U.S.A. and Department of Veterinary Clinical Sciences^d Purdue University, West Lafayette, IN 47907, U.S.A.

Received 15 June 1998; accepted 8 August 1998

Abstract: Investigation of furans, pyrroles and pyrazolones identified 3-pyridyl-2,5-diaryl-pyrroles as potent, orally bioavailable inhibitors of p38 kinase. 3-(4-pyridyl)-2-(4-fluoro-phenyl)-5-(4-methylsulfinylphenyl)-pyrrole (L-167307) reduces secondary paw swelling in the rat adjuvant arthritis model: ID₅₀ = 7.4 mg/kg/b.i.d.

© 1998 Elsevier Science Ltd. All rights reserved.

The cytokines IL-1 and TNF- α are believed to be important potentiators of the inflammatory process.² Monoclonal antibodies to TNF- α and IL-1 block acute and chronic models of inflammatory diseases in animal models. Phase 1 trials of anti-human TNF- α in patients with rheumatoid arthritis have shown improvement in various clinical measures.³ Anti-TNF- α has also been shown to be effective in Crohn's disease. Potentiated levels of IL-1 β in inflammatory arthritis and its ability to cause greater cartilage damage than TNF- α suggests that inhibition of the action of both of these cytokines may provide a useful treatment for inflammatory disorders.

Recently, a series of substituted imidazoles were identified as inhibitors of LPS stimulated human monocyte IL-1 and TNF- α production.⁴ SB 203580 was identified by structural modification of SKF 86002, which in turn was developed by hybridization of the structures of Flumizole or Triflamizole and Levamisole (Figure 1).⁵ The molecular target of SKF 86002 was identified as a pair of closely related mitogen activated protein kinase homologues (p38).⁴ SB 203580 has been shown to be effective in several models of cytokine inhibition and inflammatory disease.⁶

The developmental route to SB 203580 (Figure 1) suggested that the imidazole scaffold of this series was not critical for inhibition of p38 kinase.⁵ SmithKline had reported that SKF 86055, the regioisomer of SKF 86002, had considerably reduced potency in the inhibition of IL-1 β and TNF- α production by human monocytes. This result suggested that heterocycles stable as regioisomers (in contrast to the tautomeric imidazoles) should be investigated with the goal of identifying an analog with advantages over SB 203580.⁷ Furan, pyrrole and pyrazolone heterocycles were chosen as possible alternatives to the imidazole scaffold. We wish to report our initial results that have led to the identification of a potent pyrrole based inhibitor of p38 kinase, L-167307, **1**.⁸

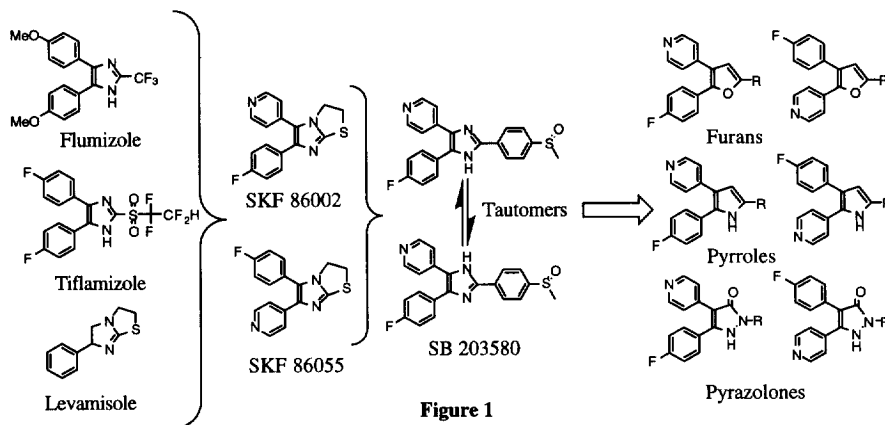
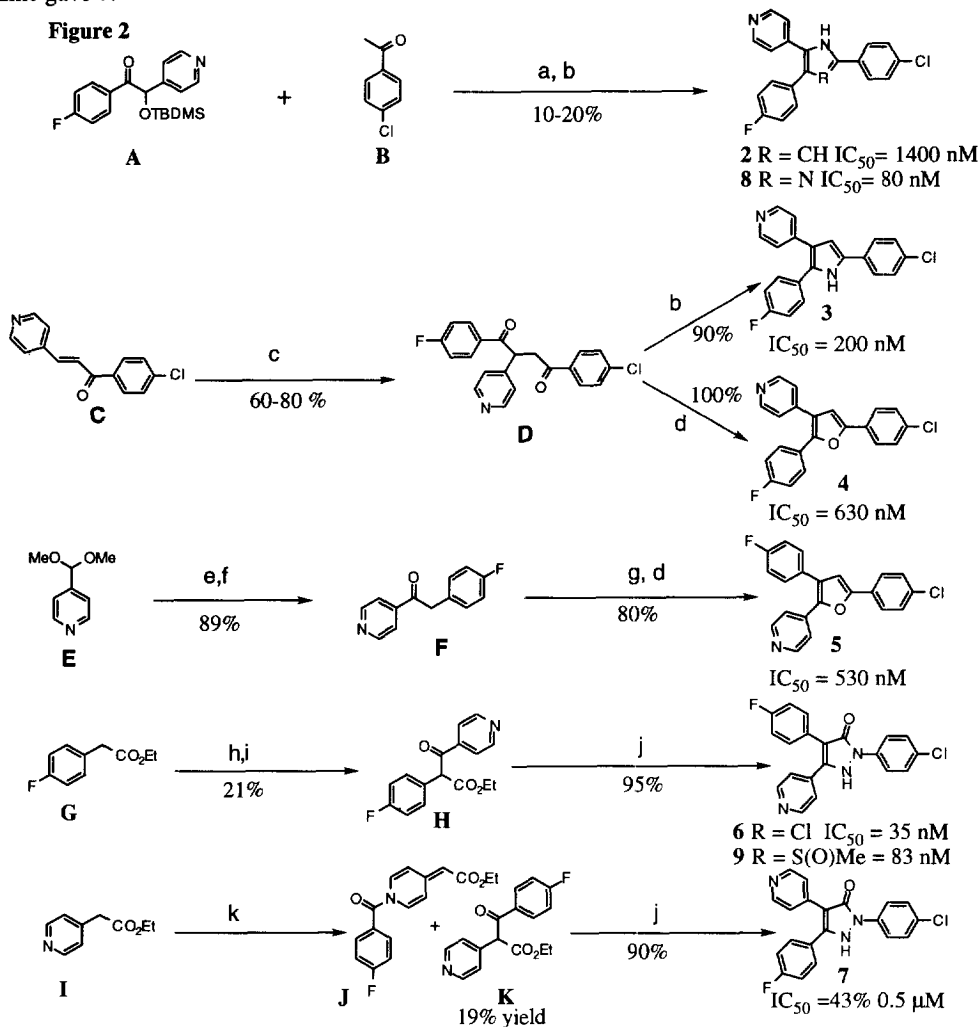


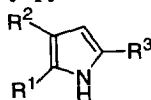
Figure 1

Chemistry

Specific examples of syntheses are illustrated below. Analogs were prepared by adaptation of these methods.⁹ The imidazole SB203580 was prepared by oxidation of the 2-(4-thiomethyl)-imidazole analog which, in turn as in the case of **8**, was derived from the benzoin **A** as described in the literature.¹⁰ **2** was prepared by condensation of benzoin **A** with acetophenone **B**.¹¹ The distal pyrrole regioisomer **3** was prepared via Paal-Knorr condensation of **D**. The 1,4-diketones **D** were available by Stetter reaction of aldehydes with chalcones **C**.¹² The 3-pyridyl-furan **4** was prepared by acid catalysed dehydration of **D**. The 2-pyridyl furan **5** was prepared by acid catalysed dehydration of the 1,4 diketone prepared by alkylation of **F** with 2-bromo-4'-fluoroacetophenone. **F** was prepared by alkylation of the acetal **E** with 4-fluoro benzyl bromide followed by acid catalysed hydrolysis.¹³ The Knorr synthesis of pyrazolones was applied to the preparation of **6** and **7**.¹⁴ Aldol condensation of **G** with 4-pyridaldehyde followed by Swern oxidation gave the β -keto ester **H**.¹⁵ Condensation with 4-chlorophenyl hydrazine provided **6**. Acylation of the sodium enolate of **I** led to a 80:20 mixture of the N-acylated pyridine **J** and the desired β -keto ester **K**. Condensation of **K** with 4-chlorophenyl hydrazine gave **7**.



a. KCN, 90% EtOH/H₂O, reflux. b. NH₄OAc, HOAc, 110 °C. c. 4-fluorobenzaldehyde, DMF, NaCN cat. d. TsOH, PhMe, reflux. e. BuLi, THF, -78 °C, 4-F-PhCH₂Br. f. HCOOH. g. NaNTMS₂, DMSO, 4-F-PhCOCH₂Br. h. LDA, THF, -78 °C, PyrCHO. i. Swern. j. 4-ClPhNHNH₂, PhMe, reflux. k. NaNTMS₂, THF, -78 °C, 4-F-PhCOCl.

Table 1: p38 Inhibitory Potency of 3-pyridyl pyrroles

	R ¹	R ²	R ³	IC ₅₀ p38 nM
1	4-F-Ph	4-Pyr	4-S(O)Me-Ph	5.1
3	4-F-Ph	4-Pyr	4-Cl-Ph	200
10	Ph	4-Pyr	Ph	17
11	4-Cl-Ph	4-Pyr	Ph	18
12	3-Cl-Ph	4-Pyr	Ph	29
13	2-Cl-Ph	4-Pyr	Ph	500
14	4-SMe-Ph	4-Pyr	Ph	690
15	4-t-BuO-Ph	4-Pyr	Ph	>10 00
16	4-CO ₂ Et-Ph	4-Pyr	Ph	>10000
17	4-OH-Ph	4-Pyr	Ph	2400
18	4-CF ₃ -Ph	4-Pyr	Ph	910
19	4-CN-Ph	4-Pyr	Ph	450
20	3-CN-Ph	4-Pyr	Ph	53
21	4-F-Ph	4-Pyr	Ph	12
22	3,4-(F)-Ph	4-Pyr	Ph	4.4
23	2,4-(F)-Ph	4-Pyr	Ph	29
24	3,4-(Cl)-Ph	4-Pyr	Ph	30
25	4-Pyr	4-Pyr	Ph	1220
26	3-Pyr	4-Pyr	Ph	240
27	2-Pyr	4-Pyr	Ph	2300
28	2-thiophenyl	4-Pyr	Ph	120
29	3-furanyl	4-Pyr	Ph	660
30	Ph	4-Pyr	4-F-Ph	17
31	4-F-Ph	4-Pyr	4-F-Ph	60
32	Ph	4-Pyr	4-OMe-Ph	280
33	4-F-Ph	4-Pyr	4-OMe-Ph	60
34	Ph	4-Pyr	2,5-(OMe)-Ph	5000
35	4-F-Ph	4-Pyr	2,5-(OMe)-Ph	1700
36	Ph	4-Pyr	4-Cl-Ph	510
37	4-F-Ph	4-Pyr	4-Br-Ph	100
38	Ph	4-Pyr	3-F-Ph	42
39	Ph	4-Pyr	2-F-Ph	34
40	4-F-Ph	4-Pyr	4-SMe-Ph	44
41	4-F-Ph	4-Pyr	4-SO ₂ Me-Ph	9.8
42	Ph	4-Pyr	4-CO ₂ Et-Ph	130
43	Ph	4-Pyr	4-COOH-Ph	14
44	Ph	4-Pyr	4-NH ₂ -Ph	28
45	Ph	4-Pyr	4-NO ₂ -Ph	6.1
46	Ph	4-Pyr	3-NO ₂ -Ph	53
47	Ph	4-Pyr	4-(CONH(CH ₂) ₂ -1-piperidinyl)-Ph	97
48	Ph	4-Pyr	4-(NHCO(CH ₂) ₂ -1-piperidinyl)-Ph	390
49	4-F-Ph	Ph	Ph	79% @ 20 μM
50	4-F-Ph	2-Pyr	4-Cl-Ph	>10000
51	4-F-Ph	4-Pyrimidinyl	Ph	710
52	4-F-Ph	4-quinolinyl	4-SOMe-Ph	114
53	4-F-Ph	2-Me-4-Pyr	4-SOMe-Ph	6.0
54	4-F-Ph	3-Me-4-Pyr	4-SOMe-Ph	260

Investigation of Heterocyclic Modifications of SB 203580

Pyrroles, furans and pyrazolones were chosen as initial targets and the p38α IC₅₀ was compared with the imidazole **8** as a control (Figure 2).¹⁶ The potency of **8** was twofold less than SB203580. Both regioisomeric furan analogs **4** and **5** were equipotent with each other. **5** was fivefold less potent than the isosteric imidazole **8**.

4 was sevenfold less potent than the corresponding imidazole **8**. The 3-pyridyl pyrrole regioisomer **3** was seven fold more potent than the 2-pyridyl pyrrole isomer **2** and only half as potent as the imidazole analog **8**. This regioisomeric differentiation of potency was also observed for the pyrazolidinones **6** (IC_{50} = 35 nM) and **7** (IC_{50} = 43% at 0.5 μ M). However, in contrast to the pyrrole case the isomer with the pyridine ring proximal to the pyrazolidinone NH **6** was considerably more potent than the distal isomer **7**. The improved potency of isosteric pyrroles over furans suggests that the pyrrole NH directly interacts with p38. Comparison of the pyrazolone with the pyrrole indicates that a complex interaction may be occurring involving both steric, electronic and hydrogen bonding interactions.

Having established the correct regioisomer in the pyrrole and pyrazolone series for effective p38 inhibition the pyrrole and pyrazolone analogs of SB203580 were prepared in both series. The 3-pyridyl pyrrole **1** was eightfold more potent than SB203580 and the pyrazolone **9** (prepared by treatment of **H** (Figure 1) with 4-thiomethylphenylhydrazine followed by oxidation) was approximately twofold less potent than SB203580. The lack of improvement in the potency of **9** prompted us to focus on the investigation of the SAR of pyrrole **1**.

Table 1 illustrates the effect of modification of the pyrrole 2, 3 and 5 positions. The effect of modification of the 2 position is illustrated by compounds **10–29**. Comparison of **11**, **12** and **13** indicates that 3 and 4 substitution is preferred. Large 4-substituents (SMe, CO₂Et) are detrimental to potency as are polar substituents such as hydroxyl and phenyl isosteric heterocycles. The best substituents of those explored are small electron withdrawing groups such as fluorine and chlorine at the 3 and 4 positions.

Variation of the aryl substituent at the pyrrole 2 and 5 positions is illustrated by compounds **1**, **3**, **10**, **21** and **30–48**. Comparison of 2-(4-fluoro-phenyl)-pyrroles (R^1 =4-F-Ph) **21**, **31**, **33**, **35**, **3** with the corresponding 2-phenyl-pyrrole analogs (R^1 =Ph) **10**, **30**, **32**, **34**, **36** demonstrates that the fluorine substituent has little effect on potency.

Modification of the 5-aryl-pyrrole substituent where R^1 =Ph or 4-F-Ph indicates that small polar substituents maintain or improve potency (**1**, **30**, **41**, **43**, **45**) whereas larger or more lipophilic substituents reduce potency (**32**, **36**, **40**, **42**, **47** and **48**). 4 substitution is preferred over 2 or 3 substitution (**34**, **38**, **39** and **46**).

The importance of the 4-pyridyl group is demonstrated by comparison of the 3-phenyl analog **49** with **21**. The position of the nitrogen atom in the aromatic ring is also important as seen by the reduced potency of the 2-pyridyl and pyrimidinyl analogs **50** and **51**. Substitution on the pyridyl ring reduced potency in the case of the 3-methyl-pyridin-4-yl and quinolinyl analogs **54** and **52**. However the 2-methyl-pyridin-4-yl analog **53** was equipotent with 4-pyridinyl analog **1**. Of the analogs prepared, the 4-methyl sulfoxide **1** and 4-methyl sulfone **41** were explored further.

Pharmacological and Pharmacokinetic Evaluation of **1**

The *in vitro* inhibitory potency of **1** and its metabolite (vide infra) **41** was evaluated against p38 subtypes as well as a selection of other kinases (Table 2).¹⁷ **1**, **41** and SB203580 inhibit p38 β and p38 α with approximately the same potency. All three inhibitors fail to inhibit p38 γ . **1**, **41** and SB203580 are poor inhibitors of JNK subtypes and Raf kinase. In all cases the IC_{50} was > 1 μ M except for RAF kinase (**1** IC_{50} = 470 nM, **41** IC_{50} = 500 nM). The selectivity of **1** and **41** was approximately 8 fold better than that of SB203580 against RAF due to their greater p38 potency.

The functional efficacy of p38 inhibitors was determined by their ability to inhibit LPS induced TNF α release from human monocytes (Table 2, Monocyte).¹⁸ The eightfold greater p38 potency of **1** as compared with SB203580 was not reflected in the functional assay. **1** and **41** were only moderately more potent than SB203580 at inhibiting the release of TNF. This result may reflect differences in the ability of the pyrrole analogs to penetrate the cell wall and reach the cytosol, blood donor variability and the physical characteristics of the compound.

Table 2: Selectivity of **1, **41** and SB203580 IC_{50} μ M (n=1 except as stated)**

Compound	p38 α	p38 β	p38 γ	Raf	JNK1 α 1	JNK2 β 1	JNK2 α 2	TNF α release
1	0.005 (29)	0.0081	42% @ 50	0.47 (2)	16 (6)	1.5 (4)	7.61 (2)	0.065 (82)
41	0.009	0.010	37% @ 25	50% @ 1	50% @ 20 (6)	1.08	6.85	0.023 (3)
SB203580	0.039 (69)	0.078	46% @ 40	0.37 (7)	50% @ 5 (3)	0.28 (4)	1.92 (2)	0.083 (32)

The pharmacokinetics of **1** were determined in the rat (Table 3).¹⁹ The compound demonstrates nonlinear pharmacokinetics due to the oxidation of the sulfoxide **1** to the sulfone **41** (demonstrated by incubation with rat liver microsomes *in vitro*). **1** is well absorbed but rapidly cleared due to its oxidation to **41**.

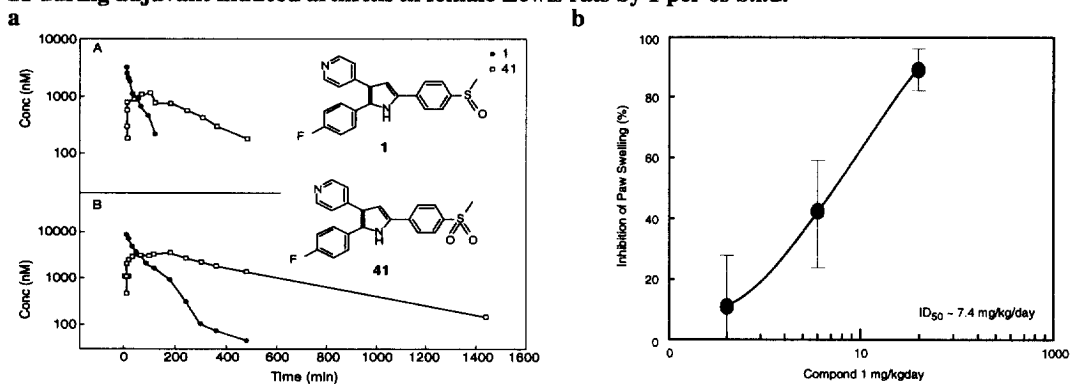
Measurement of the concentration of **1** and **41** present in plasma following dosing in rats of **1** at 2 and 5 mg/kg per os (i.v.) is illustrated in Figure 3. Rapid conversion of **1** to the sulfone is observed. The long half life of the sulfone and high plasma concentration achieved (C max, Table 3) assure that sufficient plasma concentration of drug (as **1** and **41**) is present at a dose of >2 mg/kg p.o. b.i.d to provide inhibition of p38 kinase *in vivo*.

Table 3. Pharmacokinetics of **1 following dosing in rats.**

Dose 1	CLp ml/min/kg	t1/2 min	Vdss L/kg	Auc 1 uM.hr	Auc 41 uM.hr	%F	C max uM	T max min
2 mg/kg iv	42.6	39.1	2.23	2.1 ± 0.26	6.18 ± 1.06	-	-	-
5 mg/kg iv	22.5	63.7	1.81	10.0 ± 1.5	32.56 ± 5.45	-	-	-
3 mg/kg po		122.5		0.81 ± 0.03	5.80 ± 0.49	25.6	0.31	60
10 mg/kg po		155.3		16.7 ± 5.6	95.71 ± 38.66	-	5.71	63

1 was evaluated in a rat adjuvant-induced arthritis model and compared with indomethacin as positive control and vehicle as negative control.²⁰ At the three doses investigated, the animal body weight was no different from that of vehicle treated animals. **1** reduced the secondary paw volume in a dose dependant manner with an ID₅₀ = 7.4 mg/kg/b.i.d. The ID₅₀ for SB 203580 has not been determined at this time, however, at a dose of 80 mg/kg/day 74% inhibition of reduced secondary rat foot volume was observed, as compared with 90% inhibition at a dose of 20 mg/kg/b.i.d with **1** and 79% with indomethacin at 1.0 mg/kg/b.i.d. There was less evidence of radiographic joint destruction in both hind paws with **1** at a dose of 20 mg/kg/ b.i.d than with SB 203580 at 80 mg/kg/day and indomethacin at 1.0 mg/kg/b.i.d.²¹

Figure 3. (a) Plasma Concentration-time curves of **1 and it's sulfone metabolite **41** in rats following i.v. administration of (A) 2 mg/kg and (B) 5 mg/kg **1** (n = 3). (b) Inhibition of secondary paw swelling on day 21 during adjuvant induced arthritis in female Lewis rats by **1** per os b.i.d.**



Conclusions

Furan, pyrazolone and pyrrole scaffolds were explored as replacements of the imidazole ring of SB 203580. Of these the 2,5-diaryl-3-pyridyl-pyrroles constituted a potent class of selective p38 inhibitors. **1** is eight fold more potent than SB203580 as an inhibitor of p38 kinase. However, this improved potency is not reflected in functional inhibition of TNF α production in human monocytes. **1** and its metabolite **41** inhibited secondary paw swelling in the rat adjuvant model of arthritis with an ID₅₀ = 7.4 mg/kg/day. Comparison **1** with SB203580 in the rat AIA model of arthritis suggests that **1** and it's metabolite are more potent than SB203580 but less potent than indomethacin in inhibiting joint destruction and secondary paw swelling.

1, L-167307 may constitute a useful tool with which to explore the functional relevance of inhibition of p38 kinase to arthritis.

Acknowledgement. Ms. Amy Bernick for mass spectral analysis

References

1. Present address: Amgen, Boulder, CO.
2. Dinarello, C. A. *Curr. Opin. in Immunol.* **1991**, *3*, 941.
3. Elliott, M. J.; Maini, R. N.; Feldmann, M.; Long-Fox, A.; Charles, P.; Bijl, H.; Woody, J. N. *Lancet* **1994**, *344*, 1125–1127. Elliott, M. J.; Maini, R. M.; Feldmann, M.; Kalden, J. R.; Antoni, C.; Smolen, J. S.; Leeb, B.; Breedveld, F. C.; Macfarlane, J. D.; Bijl, H.; Woody, J. N. *Lancet* **1994**, *344*, 1105.
4. Lee, J. C.; Laydon, J. T.; McDonnell, P. S.; Gallagher, T. F.; Kumar, S.; Green, D.; McNulty, D.; Blumenthal, M. J.; Heys, J. R.; Landvatter, S. W.; Strickler, J. E.; McLaughlin, M. M.; Siemens, I. R.; Fisher, S. M.; Livi, G. P.; White, J. R.; Adams, J. L.; Young, P. R. *Nature* **1994**, *372*, 739. Han, J.; Lee, J. -D.; Bibbs, L.; Ulevitch, R. J. *Science*, **1994**, *265*, 808. Rouse, J. Cohen, P.; Trigon, S.; Morange, m.; Alonso-Llamazares, A.; Zamanillo, D.; Hunt, T.; Nebreda, A. R. *Cell* **1994**, *78*, 1027.
5. Lee, J. C.; Badger, A. M.; Griswold, D. E.; Dunnington, D.; Truneh, A.; Votta, B.; White, J. R.; Young, P. R.; Bender, P. E. *Annals New York Academy of Sciences.* **1993**, *896*, 149.
6. Badger, A. M.; Bradbeer, J. N.; Votta, B.; Lee, J. C.; Adams, J. L.; Griswold, D. E. *J. Pharmacol. Exp. Ther.* **1996**, *279*, 1453.
7. Boehm, J. C.; Smietana, J. M.; Sorenson, M. E.; Garigipati, R. S.; Gallagher, T. F.; Sheldrake, P. L.; Bradbeer, J.; Badger, A. M.; Laydon, J. T.; Lee, J. C.; Hillegass, L. M.; Griswold, D. E.; Breton, J. J.; Chabot-Fletcher, M. C.; Adams, J. L. *J. Med. Chem.* **1996**, *39*, 3929.
8. Merck & Co Inc. International Patent Application WO 9705878.
9. All new compounds were analysed by high resolution NMR, HPLC and FABMS. Pyrroles in Table 2 were prepared by application of the methods described in Figure 2
10. Gallagher, T. F.; Fier-Thompson, S. M.; Garigipati, R. S.; Sorenson, M. E.; Smietana, J. M.; Lee, D.; Bender, P. E.; Lee, J. C.; Laydon, J. T.; Griswold, D. E.; Chabot-Fletcher, M. C.; Breton, J. J.; Adams, J. L. *Bioorg. Med. Chem. Lett.* **1995**, *5*, 1171. SmithKline Beecham Corporation. International Patent Application WO 93/14081
11. Ceraulo, L.; Agozzino, P.; Ferrugia, M.; Spiro, V. J. *Het. Chem.* **1990**, *27*, 255.
12. Stetter, H.; Kuhlmann, H. *Organic Reactions* **1991**, *40*, 407.
13. Sheldrake, P. W. *Synth. Commun.* **1993**, *23*, 1967.
14. Knorr, L. *Chem. Ber.* **1884**, *17*, 546.
15. Smith, A. B.; Levenberg, P. A. *Synthesis* **1981**, 567.
16. LoGrasso, P. V.; Frantz, B.; Rolando, A. M.; O'Keefe, S. J.; Hermes, J. D. and O'Neill, E. A. *J. Biochem.* **1997**, *36*, 10422.
17. Kumar, S.; McDonnell, P. C.; Gum, R. J.; Hand, A. T.; Lee, J. C. and Young, P. R. *Biochem. Biophys. Res. Commun.* **1997**, *235*, 533. Stein, B.; Yang, M. X.; Young, D. B.; Janknecht, R.; Hunter, T.; Murray, B. W. and Barbosa, M. S. *J. Biol. Chem.* **1997**, *272*, 19509. Lechner, C.; Zahalka, M. A.; Giot, J. F.; Moller, N. P. H. and Ullrich, A. *Proc. Natl. Acad. Sci. U. S. A.* **1996**, *93*, 4355. Goedert, M.; Cuenda, A.; Craxton, M.; Jakes, R. and Cohen, P. *Embo J.* **1997**, *16*, 3563.
18. Jayne Chin and Matthew J. Kostura. *J. Immun.* **1993**, *151*, 5574.
19. At each leg three fasted male Sprague-Dawley rats were dosed iv (ethanol/PEG-200 1/9)) or orally (PEG-400/water (7.5/2.5)). Blood samples were withdrawn periodically from a cannula implanted in the right jugular vein. The blood was centrifuged and the plasma treated with acetonitrile, recentrifuged and the supernatant analysed by HPLC. Bioavailability was calculated from the AUC's of the low i.v. and oral doses at 2 and 3mg/kg
20. Adjuvant-induced arthritis (AIA) was induced in 7 week old female Lewis rats (126–169 gm; n = 10) by an intradermal injection of 0.5 mg of *M. butyricum* in light mineral oil in the left hind foot pad. Body weights, radiographs and foot volumes of both paws were determined on various days (0, 4, 14 and 21). 1 (2, 6, and 20 mg/kg/day p.o. b.i.d.), Indomethacin (1 mg/kg/day p.o. b.i.d.) and vehicle (0.5% methocel) were started on day 0 and continued throughout the experiment. Blood (1 mL) was withdrawn by cardiac puncture under methoxyflurane anesthesia 1 hour or 4 hr after the last dose to determine plasma levels of 1. Rats were euthanized by carbon dioxide inhalation on day 21. The thymus and spleen of all rats were removed and weighed to assess tibio-tarsal joint integrity, radiographic scores were assigned according to an adaptation of a previously described method (Clark R. L.; Cuttino, Jr., J. T.; Anderle, S. K.; Cromatie, W. T.; Schwab, J. H. *Arth. Rheum.* **1979**, *22*, 25) by a boarded radiologist who was blinded to treatment. General necropsy noted that abdominal, peritoneal and thoracic cavities were normal. 1 demonstrated efficacy in many of the parameters examined in rat AIA (body weight, paw swelling, and thymus and spleen weights). Indomethacin inhibited the secondary paw swelling by 79% in this experiment.
21. Radiographic scores: 1 20 mg/kg/ b.i.d. 1° paw = 3.6; 2° paw = 1.6. SB 203580 80 mg/kg/day: 1° paw = 6.1; 2° paw = 2.6. Indomethacin 1.0 mg/kg/day : 1° paw = 4.9; 2° paw = 2.9.